Methods and Equipment for Complex Investigation of Modified Surface Layers and Coatings

I.B. Stepanov, I.A. Shulepov, D.O. Sivin, S.E. Eremin

Nuclear Physics Institute, 2a, Lenin Ave., Tomsk 634050, Russia

Abstract – A review of the equipment and methods of investigating elemental composition and physicomechanical properties of surface layers of materials and coatings used at the Scientific Research Nuclear Physics Institute (Tomsk) is presented. The special features of application of atomic and nuclear physics methods of investigating the elemental composition versus the depth of ion-modified layers of materials and coatings are considered. Results of integrated studies of the surface morphology, tribological characteristics, nanohardness, and adhesion strength of coatings and ion-modified surface layers of materials are presented.

1. Introduction

Nowadays interest in the study of solid body surfaces grows steadily. This is explained by the fact that physical and chemical properties of thin surface layers determine such characteristics of materials as strength, temperature stability and corrosion resistance, friction, wear, and dielectric and decorative characteristics. Numerous methods of ion modification of the surface and surface layers of a solid body and coating deposition are developed. In this regard, comprehensive information on the acquired properties of the surface and surface layers of solid bodies is required. Under the comprehensive information is meant information on the elemental composition of the surface and surface layers, chemical bonds of atoms, mechanical and tribological characteristics, surface morphology, changes in phase composition, microstructure, and thickness of the modified layers, and adhesive properties of coatings.

In the present study, results of investigations of $TiAl_xN_y$ coatings formed using the NNV6,6-I1 installation intended for deposition of ion-plasma coatings and equipped with a system for microdrop fraction removal from the plasma and with the PINK gas plasma generator are presented. The TiNi and AlTi intermetallic layers were formed using the Raduga-5 ion source.

To prepare samples, a Brillant 201 cutting lathe and a Saphir 320E automated grinding-polishing lathe were used. The given equipment allows the plain polished surface of samples of metals, alloys (including solid ones), ceramics, semiconductors, etc. to be prepared for 1.5–2 h with roughness Rz=0.1 μm.

2. Adhesion strength of films and coatings

Figure 1 shows the measured adhesion strength of the $TiAl_xN_y$ coating. Investigations were carried out by the scratch method with an MST-S-AX-0000 device. The equipment operated in the mode of controllable drawing of a scratch under loading that changed with time. The loading/resolution ratio was in the range (0.1 mN–30 N)/0.1 mN. The maximum scratch length was 20 mm. The indenter diameters were 40, 200, and 800 μm. The given method allows the adhesion strength of coatings deposited in different technological modes to be measured.

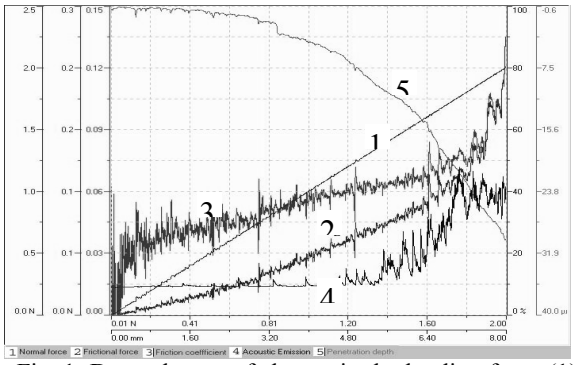

Fig. 1. Dependences of change in the loading force (1), resistance force (2), resistance coefficient (3), acoustic emission (4), and indenter penetration depth (5) on the scratch length

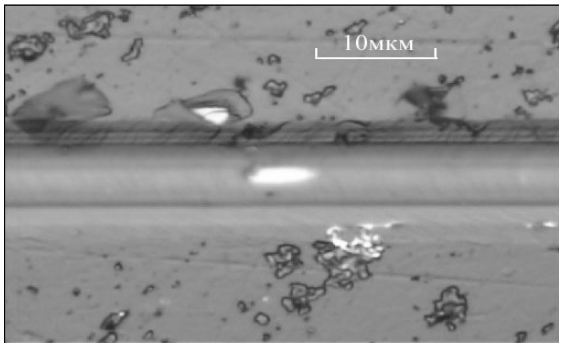

Fig. 2. Image of a scratch from an indenter on the $TiAl_xN_y$ coating surface

An analysis of curve shapes together with microscopic scratch images (Fig. 2) allows the instant of coating destruction (cracking, spalling, swelling, etc.) to

be identified. For the case illustrated by Fig. 1, spalling of the $TiAl_xN_y$ coating from the HSS substrate was observed under indentor loading of 1.3 N, which is clearly seen from the acoustic emission curve.

3. Nanohardness and the Young modulus

Fig. 3 shows the measured nanohardness and the Young modulus of the $TiAl_xN_y$ coating under the action of a diamond indenter with a load of 66.2 mN. The indenter penetration depth was 400 nm.

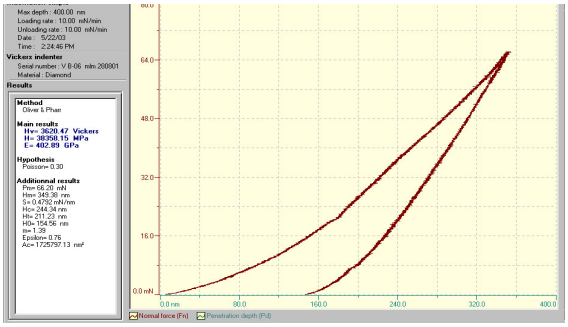

Fig. 3. Loading-unloading curves under the action of indenter on the $TiAl_xN_y$ coating surface

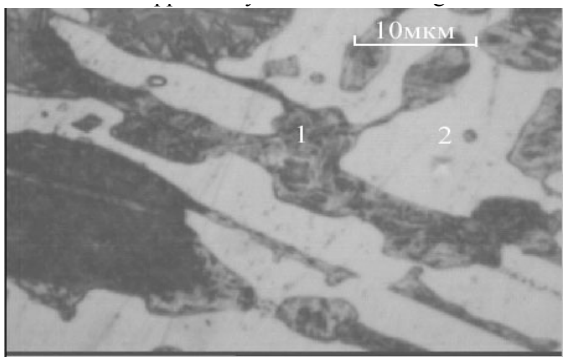

Fig. 4. Image of the surface of coating formed by an electron beam with indentations (1 and 2) from the Vickers indenter

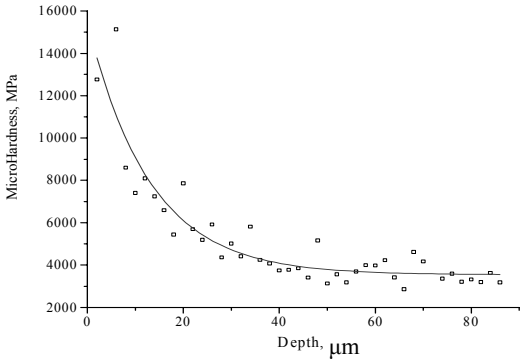

Fig. 5. Change of nanohardness with depth for the coating-substrate interface

Investigations were carried out with an NHT-S-AX-000H Nanohardness Tester. The characteristics of the equipment allow measurements to be carried out to depths as great as 20 μm with resolutions up to 0.03 μm. Loads were changed from 0.8 to 300 mN with a step of ± 1 μN. The device was equipped with a microscope at 50×, 200×, and 1000× magnification and a digital videocamera.

High resolution of the device provided the opportunity of measuring the nanohardness of individual grains and intergranular space as well as of depth scanning of the modified layer. Figure 4 illustrates the opportunity of indentation of grains crystallized during ion-beam coating deposition, and Fig. 5 shows the results of depth scanning of the coating-substrate interface of the transverse sample with a step of 2 μm.

4. Tribological characteristics of materials and coatings

The basic tribological characteristics of the coating and modified surface layers of materials are the friction coefficient and wear resistance. In the present study, a THT-S-AX0000 high-temperature tribometer was used to analyze the tribological characteristics. The device allowed the friction coefficient and wear intensity to be measured with the use of methods standardized to DIN 50324 by the ball-on-disk and needle-on-disk methods.

The device operation is based on the study of the wear track formed under the action of the rest indenter on the rotating sample. The device specifications provided the shaft rotation frequency changing in the range (1–1500) rev/min with a maximum angular momentum of 450 N mm and friction force up to 10 N. The secific feature of the device was the opportunity of carrying out tribological investigations of samples at temperatures up to 1000 K. Investigations can be carried out in lubricating liquids or in inert gas media.

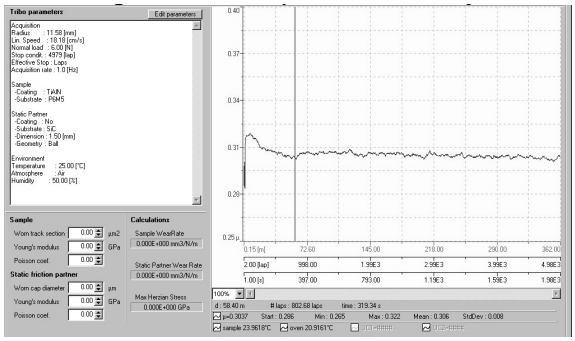

Fig. 6. Dependences of change in wear intensity and friction coefficient for ion-modified layers and initial Ti and Ni targets vs. their temperature

Fig. 6 shows diagrams of change in wear intensity for initial and implanted targets for Al →Ti and Ti→Ni systems. When the sample temperature increases to 700 K, one can observe a sharp increase in the wear intensity by a factor of 2.5 for the initial Ti and Ni targets. For ion-implanted surface layers, the dependence of change in wear intensity on the temperature is not observed. In this case, intermetallic phases formed in the surface layers demonstrate their anomalously high temperature properties. Oxide and carbide phases formed on the sample surface also decrease the wear.

High exploitation properties of Al→Ti and Ti→Ni intermetallic systems were revealed in experiments on measuring the friction coefficient (Fig. 6). For the Al→Ti system, change in friction coefficient with increase in temperature is within the measurement error. At the same time, the friction coefficient of initial titanium increases by a factor of 1.5. One more regularity was revealed when investigating the Ni target. The physical properties of this material in the initial state determine its low friction coefficient. With increase in the temperature, the Ni friction coefficient decreases by a factor of 1.4. Unlike initial Ni, the Ti→Ni system undergoes smaller temperature changes. Nevertheless, the friction coefficient decreases with increase in temperature and remains less than for the Al→Ti system.

5. 3D contactless profilometry

Investigations of the surface morphology are one of the most important problems in the development of new modes of ion-beam and plasma modification of the properties of materials. One of the methods of analyzing the geometrical characteristics of the material surface is the 3D contactless profilometry. Figure 7 (1) shows an image of the $TiAl_xN_y$ coating surface recorded with a Micro Measure 3D Station. The ($X\times Y$) scanning area was 100×100 mm^2 with resolutions up to 0.1 mm along the X and Y axes and up to 1 nm along the Z axis. The software of the device allowed more than 200 calculation and statistical functions to be realized.

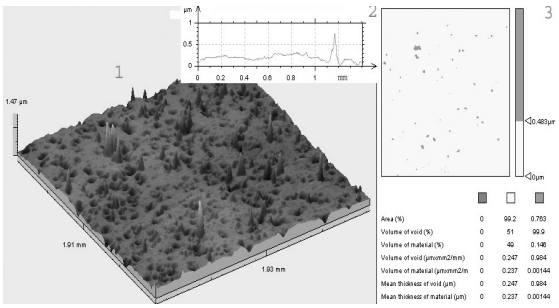

Fig. 7. 3D image of the TiAlxNy coating surface (1), roughness measurements (2), and diagram of microdrop fraction distribution over the coating surface (3)

Figure 7 (2) shows the roughness measured for the coating. From the figure it can be seen that the surface roughness does not exceed Rz=0.64 μm for the substrate roughness Rz=0.4 μm and coating deposition using continuous vacuum-arc plasma with removed microdrop fraction.

As an example of realization of a statistical function, Fig. 7 (3) shows a diagram of microparticle size distribution as a ratio of the area occupied by microparticles of the given sizes to the area of the examined surface. Based on the data of Fig. 7 (3), we can conclude that removal of microdrop fraction from the vacuum-arc plasma allows the microparticle content on the examined surface to be decreased by more than 10^3 times.

6. Coating thickness

Nowadays new original methods of rapid analysis arise in addition to the conventional (profilometric and microscopic) methods of measuring the coating thickness. One of such methods is based on an analysis of widths of spherical sample sectors.

Figure 8 shows an example of realization of this method. The Cat-S-AX-0000 Calotest was used to prepare a spherical sample. The principle of the device operation is based on attrition of the coating by a ball with a preset diameter in the presence of an aqueous solution of diamond dust at the contact point. The ball diameter allows the coating thickness to be determined with resolution up to 0.1 μm. In this case, the measurement time, as a rule, does not exceed 0.5–1 min.

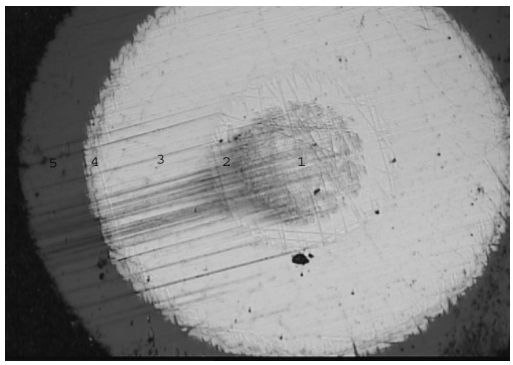

Fig. 8. Spherical sample: (1) multilayered coating of a substrate from the VK-8 alloy, (2) TiN, (3) TiC, (4) TiN, and (5) Al_2O_3

As can be seen from Fig. 8, the method allows thicknesses of multilayered coatings to be easily determined. An analysis of the elemental composition by the method of Auger electron spectrometry demonstrates that the examined sample comprises a substrate from VK-8 alloy (1), TiN layer with thickness of 0.7 μm (2), TiC layer with thickness of 3.4 μm (3), TiN layer with thickness of 0.5 μm (4), and Al_2O_3 layer with thickness of 3.2 μm (5).

7. Auger electron spectrometry (AES)

In the last few years the Auger electron spectrometry has recommended itself as one of the universal and most convenient methods of measuring the concentration of elements in the surface layers of materials and coatings.

Figure 9 shows the depth profiles of element distribution for the $TiAl_xN_y$ coating. The results were obtained using the Shkhuna-2 Auger spectrometer. The depth resolution of the spectrometer reached 0.5–1 nm.

The data shown in Fig. 9 vividly demonstrate the formation of the coating 0.7 μm thick on the HSS substrate. An analysis of the results obtained allows us to conclude that Al in two phases (AlN and Ti_xAl_y) is presented in the coating.

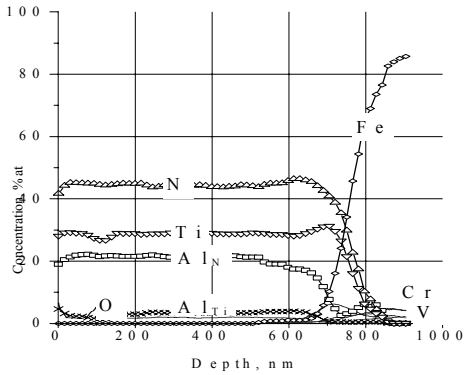

Fig. 9. Depth profiles of element concentration distribution for the $TiAl_xN_y$ coating

8. Rutherford backscattering (RBS)

The RBS method was realized on the basis of an electrostatic accelerator with ion beam energy of 1 MeV. The method allowed profiles of element concentration distribution with the sample depth and at the interface between the examined sample layers to be recorded with sensitivity up to (0.1–0.5) at.% without sample estruction for a short time.

As an example of realization of the RBS method, Fig. 10, *a* shows the profile of element concentration distribution for the TiNi intermetallic layer. Fig. 10, *b* shows the registered and model (solid enveloping curve) energy spectra and individual partial spectra of the examined elements.

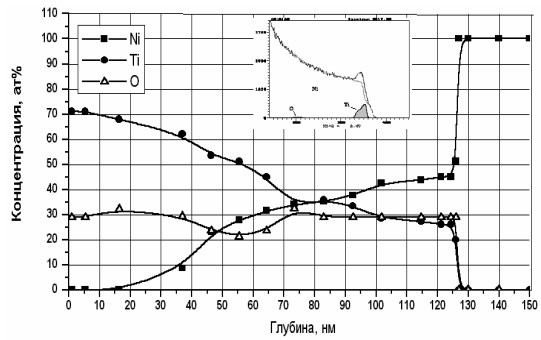

Fig. 10. Depth profiles of element concentration distribution for the Ni surface layer

9. Analysis of small element concentrations

The method of atomic emission spectrum analysis is best suited for solving problems connected with the determination of small concentrations of elements. One of the most widespread devices realizing the given method of analysis is a DFS-458S spectrometer equipped with a photo-electric attachment. The device registers spectra of samples without omissions with position-sensitive linear radiation detectors. The device operation and measurement data processing are computer-controlled.

The sensitivity to individual elements of the examined material measured with the DSF-458S complex reaches 10^{-4}–10^{-6} %. Unlike the well-known devices used to investigate the elemental composition of materials, the DFS-458S complex allows samples to be analyzed without their preliminary preparation with the material composition kept unchanged thereby ensuring correctness of the results obtained.

A method of quantitative atomic emission element analysis of materials without reference samples has been developed on the basis of the DFS-458S complex. The method is based on elimination of uncontrollable factors that influence the spectral line intensities when implementing the algorithm of normalizing the spectrum intensity. The error in measuring the elemental composition of pure metals (Ni, Co, and Cu) and steels (P6M5 and VK9) by the developed method, in comparison with the method of determining the element concentration with the use of reference samples, does not exceed a few percent.

10. Conclusions

he developed complex of analytical equipment and investigation methods realize a wide class of investigations of physical and exploitation properties of surface layers of materials and coatings including:

1. measurement of element concentration in surface layers of materials and coatings;
2. analysis of multilayered coating thickness;
3. surface microscopy;
4. investigations of the tribological properties of materials and coatings under changes in the temperature of samples, including measurements in lubricating liquids and inert gases;
5. measurements of nanohardness and Young's modulus of coatings and ion-modified layers of materials,
6. investigations of adhesion strength of coatings;
7. studies of the surface morphology including statistical data processing.

With the use of the analytical complex, we have established the following:

– formation of the $TiAl_xN_y$ coatings with hardness up to 38,350 MPa under the joint action of gas-discharge and continuous vacuum-arc plasmas cleaned from microdrop fraction;
– adhesion strength of the TiN coating formed under conditions of microdrop fraction removal from the plasma is by a factor of 1.7 higher than for coatings formed by conventional methods;
– axisymmetric filters with venetian-blind structure for vacuum-arc plasma filtering provide a decrease of microparticles on the coating surface 10^2–10^3 times;
– the TiNi and AlTi intermetallic systems formed in the mode of high-intensity ion implantation keep high tribological properties unchanged when the temperature increases up to 700 K;
– the best nanohardness and wear resistance characteristics of the $TiAl_xN_y$ coating correspond to the TiAlN stoichiometric composition.